

## Propagation of hydrogen-air detonation in tube with obstacles

Wojciech Rudy \*, Rafał Porowski\*, Andrzej Teodorczyk\*

*Institute of Heat Engineering, Warsaw University of Technology  
21/25 Nowowiejska Street, 00-665 Warsaw, Poland*

### Abstract

An experimental and computational study of flame propagation, acceleration and transition to detonation in stoichiometric hydrogen-air mixtures in 6 m long tube filled with obstacles located at different configurations was performed. The initial conditions of the hydrogen-air mixtures were 0.1 MPa and 293 K. Four different cases of obstacle blockage ratio (BR) 0.7, 0.6, 0.5 and 0.4 and three cases of obstacle spacing were used. The wave propagation was monitored by piezoelectric pressure transducers PCB. Pressure transducers were located at different positions along the channel to collect data concerning detonation propagation. Tested mixtures were ignited by a weak electric spark at one end of the tube. In order to support the experimental results we performed series of CFD simulations for the same conditions of hydrogen-air mixtures and the geometry of the tube. The simulation tool used in this study was a two-dimensional DETO2D code, dedicated to simulate the propagation of gaseous detonations in complex geometries.

**Keywords:** Detonation, Hydrogen Combustion, Numerical Simulation, DETO2D

### 1. Experimental set-up

The study was performed in 6 m long circular cross section tube with inner diameter  $D = 140$  mm. All tested mixtures were stoichiometric hydrogen-air mixtures with initial conditions of 0.1 MPa and 293 K. The wave propagation was monitored by piezoelectric pressure transducers PCB. Pressure transducers were located at different positions along the channel to collect data concerning detonation development. Scheme of the experimental set-up is shown in Fig. 1 and its view in Fig. 2. Tested mixtures were ignited by a weak electric spark at one end of the tube. Gas mixtures were produced using the partial pressure method and mixed by in a cylinder.

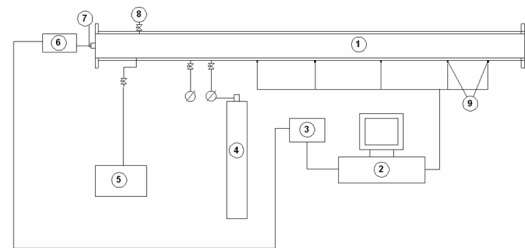


Figure 1: Experimental set-up: 1 – detonation tube, 2 – PC and data acquisition system, 3 – time sequencer, 4 – hydrogen -air cylinder, 5 – vacuum pump, 6 – ignition device, 7 – ignitron plug, 8 – dilution valve, 9 – pressure transducers

After sufficient time the gas mixture was introduced to the experimental tube, to the desired pressure.

Experimental tube consisted of four sections ( $2 \times 2$  m and  $2 \times 1$  m) jointed together and equipped

\*Corresponding author

Email addresses: wrudy@itc.pw.edu.pl (Wojciech Rudy), rporowski@gmail.com (Rafał Porowski), atead@itc.pw.edu.pl (Andrzej Teodorczyk)

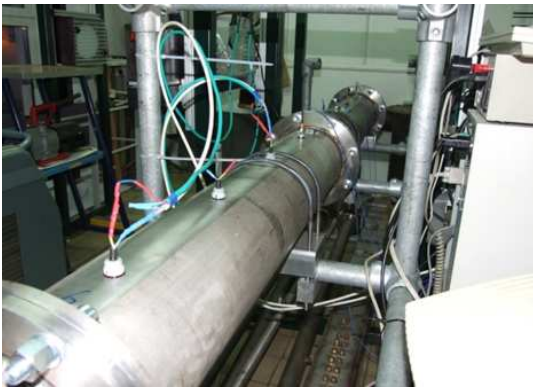


Figure 2: Photos of experimental facility

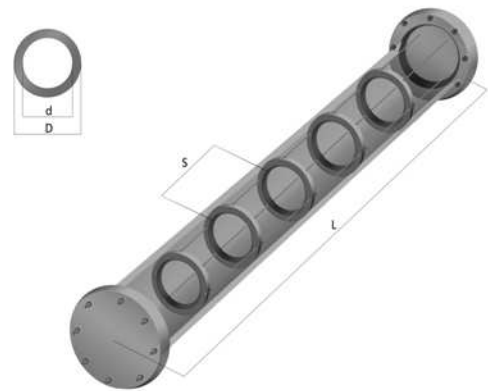


Figure 3: Schematic location of obstacles along the tube and the view of obstacles in the front of experimental tube

with different configurations of obstructions inside. Configurations of obstacles were used with blockage ratio (BR) from 0.4 to 0.7. Internal diameters of particular obstacles were chosen between 77 mm up to 108 mm and numbers of obstacles varied from 12 to 35. Obstacles inside the tube were located at various distances  $S$  which were equal to  $1 \times D = 140$  mm,  $2 \times D = 280$  mm and  $3 \times D = 420$  mm. Figure 3 shows the schematic location of obstacles along the tube as well as configuration of obstacles used in the experimental study.

The obstacles were connected by steel 5 mm in diameter rods to keep correct spacing. The influence of the rods on flame acceleration and detonation transition were not investigated.

The mechanism of deflagration-to-detonation transition in hydrogen-air mixtures was experimentally investigated in obstructed channel using pressure profiles, wave velocities and numerical calculations.

## 2. Results and discussion

Figure 4 shows the average wave velocity along the tube for hydrogen-air mixtures for the spacing between obstacles  $S = 1D, 2D, 3D$  and BR ranging from 0.4 to 0.7. As it may be observed spacing between obstacles has very visible influence on detonation velocity stability. The higher the spacing is, the lower differences between velocities are for different blockage ratios. This correlation is visible in Fig. 5 which presents percentage difference in velocity for different spacing and BR. For BR = 0.6 and 0.7 spacing influence on percentage difference in velocity is very high and gives values in range of 6–21%. For blockage ratios 0.4 and 0.5 the same parameter changes in range of 3–7%.

Figure 6 shows the pressure profiles versus time at eight locations of PCB pressure gauges along the tube for stoichiometric hydrogen-air mixture including BR = 0.4 and 0.5 with distance between obstacles  $S = 3D$  in both cases. According to our results the maximum experimental pressure at the propagating

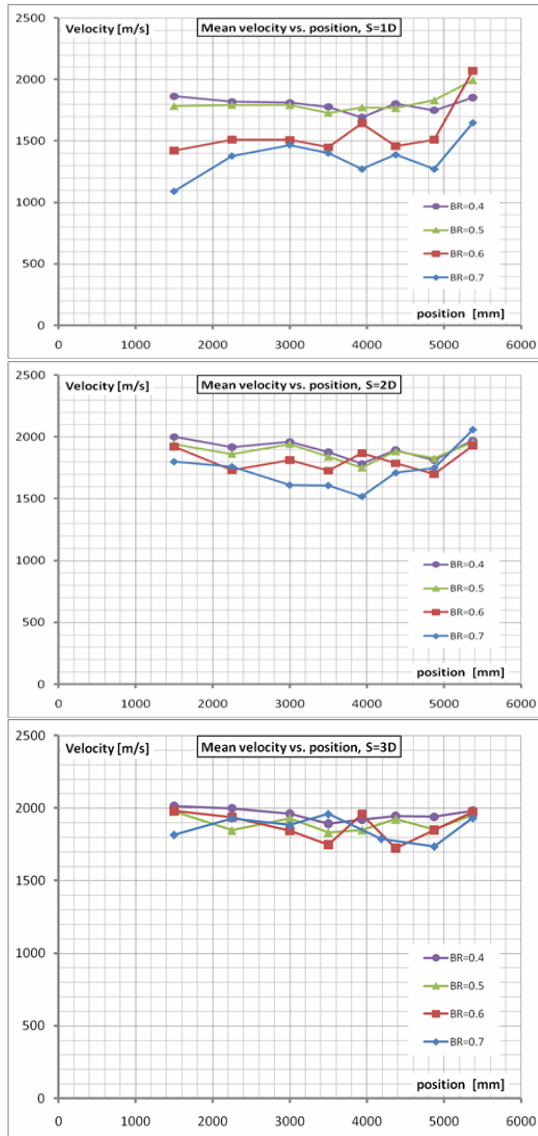


Figure 4: Experimental wave velocities of stoichiometric hydrogen-air mixtures for BR range from 0.4 to 0.7 and distance between obstacles  $S = 1D, 2D, 3D$

shock front in the driven section was slightly higher than calculated value, reaching the maximum value, approx. 3 MPa.

This pressure value was observed at the same distance where detonation wave reached the stable propagating regime. The same distance from the ignition point, as in the velocity measurements, was a so-called run-up distance for the onset of detonation in our experiments. The propagating detonation wave became a stable at the time up to 2.5 ms traveling more than 5 m from the initiation point. The last

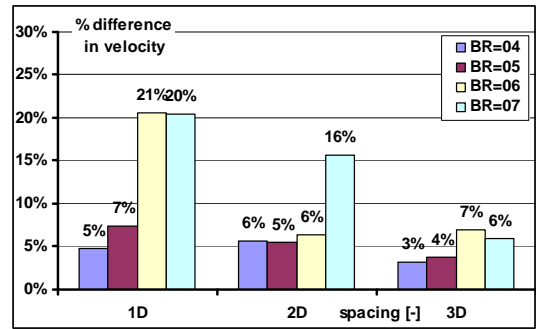


Figure 5: Percentage difference in velocity for different spacing and BR. % difference in velocity =  $((V_{max} - V_{min}) / 2) / V_{mean}$

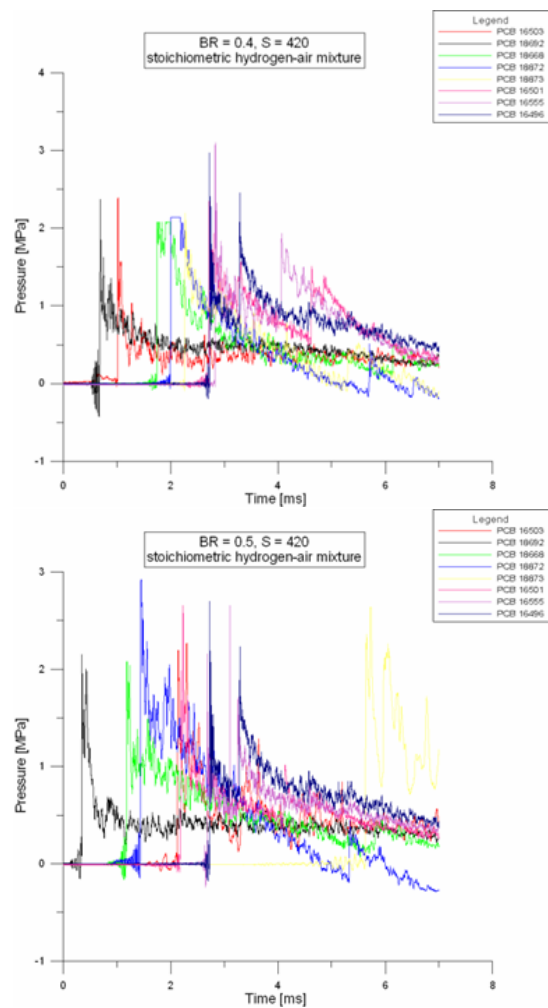


Figure 6: Pressure profiles versus time of stoichiometric hydrogen-air mixtures for BR = 0.4 and 0.5 with distance between obstacles  $S = 420$  mm

pressure gauge located at the distance about 5.4 m recorded the arrived shock front at the time close to 2 ms leaving a distance about 0.6 m from the end of

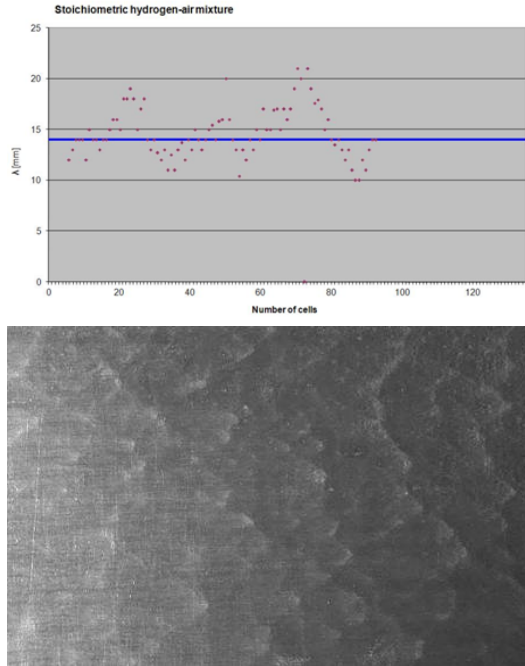


Figure 7: Detonation cell sizes for hydrogen-air mixture

the tube.

During our experiments the detonation cell sizes were measured using smoked foil technique and analyzed with Matlab image processing toolbox. The average detonation cell size recorded on the smoked foil during experiment was calculated with 2D Fourier transform written by Hebral and Shepherd [1], as the subscript for Matlab application. The cell size for stoichiometric  $H_2$ -air mixture in our experimental set-up was 14 mm.

Figure 7 shows the cell sizes versus number of cells for the case of stoichiometric hydrogen-air mixture, including  $BR = 0.5$  and distance between obstacles  $S = 420$  mm. The blue line in Fig. 7 shows the average detonation cellsize which was equal to 14 mm, based on our image processing calculations. Picture in Fig. 7 presents the smoked foil with the detonation cell pattern of the same case.

### 3. Numerical simulations

In order to support the experimental results we performed series of CFD simulations for the same conditions of hydrogen-air mixtures and the geometry of the tube. The simulation tool used in this study was an in-house two-dimensional DETO2D code,

dedicated to simulate the propagation of gaseous detonations in complex 2D geometries which may be considered as a flat 2D, axisymmetrical (cylindrical) or spherical.

#### 3.1. Mathematical model

The general form of Euler equation solved numerically in DETO2D is expressed as:

$$\frac{\partial \phi}{\partial t} + \frac{\partial}{\partial x} E + \frac{\partial}{\partial y} F = S \quad (1)$$

where:

$$\phi = \begin{pmatrix} \rho \\ \rho Y_s \\ \rho u \\ \rho v \\ \rho e \end{pmatrix}$$

$$E = \begin{pmatrix} \rho u \\ \rho u Y_s \\ \rho u^2 + p \\ \rho uv \\ \rho u \left( e + \frac{p}{\rho} \right) \end{pmatrix}$$

$$F = \begin{pmatrix} \rho v \\ \rho v Y_s \\ \rho v u \\ \rho v^2 + p \\ \rho v \left( e + \frac{p}{\rho} \right) \end{pmatrix}$$

$$S = \begin{pmatrix} 0 \\ -w_s \\ 0 \\ 0 \\ 0 \end{pmatrix} \quad (2)$$

To solve the above system of equation, operator split method is adopted. The original conservation equations can be split into the following equations:

$$\frac{\partial \phi}{\partial t} + \frac{\partial}{\partial x} E = 0 \quad (3)$$

$$\frac{\partial \phi}{\partial t} + \frac{\partial}{\partial y} F = 0 \quad (4)$$

$$\frac{d(\rho Y_s)}{dt} = -w_s \quad (5)$$

Chemical reaction model may be modeled as:

- 1-step irreversible reaction model based on Arrhenius Law,

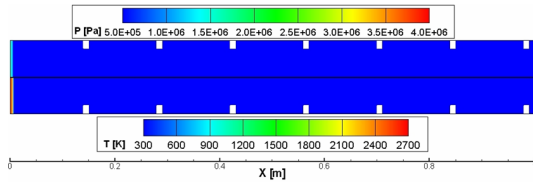


Figure 8: Initial conditions of the simulation (for better visibility only 1m long part is present)

## 2. Detailed chemical reaction model solved by VODE package included in CHEMKIN-II.

In this study full chemical reaction model was considered. The mechanism consisted of 24 reactions with  $\text{NO}_x$  formation included. Detailed data of the mechanism are presented in Table 1.

The mechanism was downloaded from Explosion Dynamics Laboratory database which is available online [2].

### 3.2. Computational domain

The computational domain was 4 m long, axisymmetric of 0.14 m in diameter geometry with obstacles spacing  $S = 1D$  and blockage ratio  $BR = 0.4$  which corresponds to the obstacles inner diameter equal of 108 mm. The gas was stoichiometric hydrogen-air mixture. The detonation was initiated by patching the region with high temperature (2,500 K) and pressure (1.6 MPa) at one side of the channel. As the geometry was axisymmetrical, only one half of the tube was under consideration. The scheme presented below (Fig. 8) shows a 1 m long part of the tube at the initial time  $\tau = 0.0$  s. The symmetrical part of the tube was added during postprocessing. This kind of postprocessing let the user to display two different parameters at the same time as it is shown in Fig. 8 where both pressure and temperature values are displayed.

### 3.3. Results

Figures 9 and 10 show numerical plots stack of 0.6 m long part of the channel at the beginning of the flow. Parameters displayed and color scale are the same as in Fig. 8. The time difference between slices is  $\Delta\tau = 5.0 \mu\text{s}$ . The time of calculations showed in these figures is 290.0  $\mu\text{s}$ . The initial conditions at the left end of the channel with

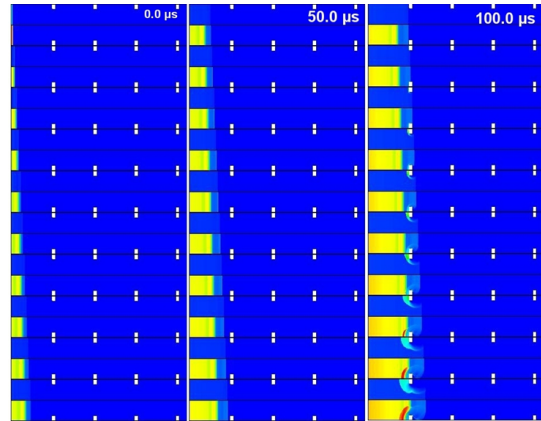


Figure 9: Results plots stack of pressure and temperature contour for time range 0.0–145.0  $\mu\text{s}$  (scale as in Fig. 8). 0.6 m long part of the channel

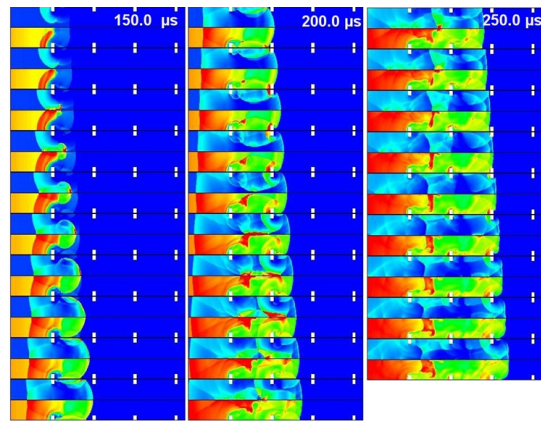


Figure 10: Results plots stack of pressure and temperature contour for time range 150.0–290.0  $\mu\text{s}$  (scale as in Fig. 8). 0.6 m long part of the channel

$T = 2,500$  K and  $P = 1.6$  MPa do not provide direct initiation of detonation. At the very beginning of the simulation shock and flame front separation may be observed. This separation is being observed for about 155  $\mu\text{s}$ . At the time of 160  $\mu\text{s}$  the shock wave reflecting from the channel walls and obstacles focuses in the centre of the channel and generates area with high pressure and temperature (approximately 4.0 MPa and 2,000 K) which generates local explosion. Detonation front generated by explosion moves with high velocity of about 2,500 m/s, catches up with leading shock and propagates at constant velocity of 2,050 m/s. For confirmation of that processes Fig. 11 is presented with wide range of results where these three processes are clearly visible. The black line corresponding to the reaction front has 3 differ-

Table 1: Detailed chemical mechanism for hydrogen-air combustion

No	Reaction	$A$	$n$	$E_a$
1	$H_2+O_2 \rightleftharpoons 2OH$	1.7000E+13	0.00	47780
2	$OH+H_2 \rightleftharpoons H_2O+H$	1.1700E+09	1.3	3626
3	$O+OH \rightleftharpoons O_2+H$	4.0000E+14	-0.5	0
4	$O+H_2 \rightleftharpoons OH+H$	5.0600E+04	2.67	6290
5	$H+O_2+M \rightleftharpoons HO_2+M$	3.6100E+17	-0.72	0
6	$OH+HO_2 \rightleftharpoons H_2O+O_2$	7.5000E+12	0.0	0
7	$H+HO_2 \rightleftharpoons 2OH$	1.4000E+14	0.0	1073
8	$O+HO_2 \rightleftharpoons O_2+OH$	1.4000E+13	0.0	1073
9	$2OH \rightleftharpoons O+H_2O$	6.0000E+08	1.3	0
10	$H+H+M \rightleftharpoons H_2+M$	1.0000E+18	-1.0	0
11	$H+H+H_2 \rightleftharpoons H_2+H_2$	9.2000E+16	-0.6	0
12	$H+H+H_2O \rightleftharpoons H_2+H_2O$	6.0000E+19	-1.25	0
13	$H+OH+M \rightleftharpoons H_2O+M$	1.6000E+22	-2.0	0
14	$H+O+M \rightleftharpoons OH+M$	6.2000E+16	-0.6	0
15	$O+O+M \rightleftharpoons O_2+M$	1.8900E+13	0.0	-1788
16	$H+HO_2 \rightleftharpoons H_2+O_2$	1.2500E+13	0.0	0
17	$HO_2+HO_2 \rightleftharpoons H_2O_2+O_2$	2.0000E+12	0.0	0
18	$H_2O_2+M \rightleftharpoons OH+OH+M$	1.3000E+17	0.0	45500
19	$H_2O_2+H \rightleftharpoons HO_2+H_2$	1.6000E+12	0.0	3800
20	$H_2O_2+OH \rightleftharpoons H_2O+HO_2$	1.0000E+13	0.0	1800
21	$O+N_2 \rightleftharpoons NO+N$	1.4000E+14	0.0	75800
22	$N+O_2 \rightleftharpoons NO+O$	6.4000E+09	1.0	6280
23	$OH+N \rightleftharpoons NO+H$	4.0000E+13	0.0	0
24	$N_2+M \rightleftharpoons N+N+M$	3.7100E+21	-1.6	224928

ent slopes. One can say that local explosion is DDT but the code does not include any viscosity effects of the gas as it is based on Euler equations.

Figure 14 shows numerical results of velocity with comparison to experimental one for  $BR = 0.4$ . There are two numerical results where one corresponds to the position of the sensors in experimental part and second corresponds to sensors directly between the obstacles (spacing equal 0.14 m). This comparison of ‘sensors density’ was made to check if there are any differences in local velocity during the detonation front propagation. As it may be seen in Fig. 14 the differences between computed velocities in both approaches differ slightly and detonation velocity is stable at about 2,050 m/s. The local velocity of 2,500 m/s is present at the beginning of the channel as it was mentioned before. Additionally, calculations of Chapman-Jouguet detonation velocity were done with STANJAN code. STANJAN calculations

brought the C-J velocity of 1,968 m/s. The comparison between DETO2D calculations and STANJAN shows that numerical velocity is overestimated for about 100 m/s (~5%) to ideal C-J velocity. To present wave position density gradient parameter is also presented in Fig. 13. After many shocks reflections the detonation front develops complicated structures of pressure waves moving ahead and backward of the channel. These pressure waves are indicated by pressure sensors in experimental and numerical cases shown in Fig. 14. As computed velocity is higher than experimental, numerical sensors indicate detonation in shorter time than experimental one.

#### 4. Conclusions

An experimental and computational study of flame propagation, acceleration and transition to detona-

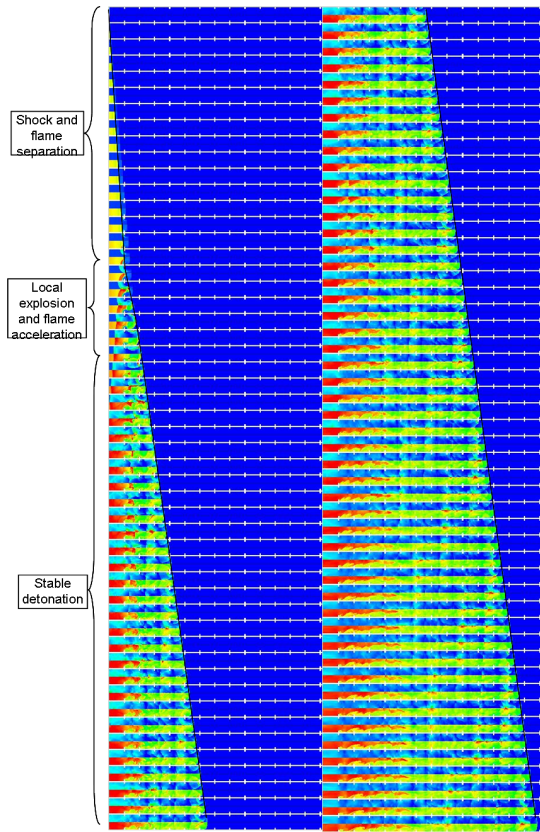


Figure 11: Results plots stack of pressure and temperature contours (scale as in Fig. 8), 2 m long part of the channel

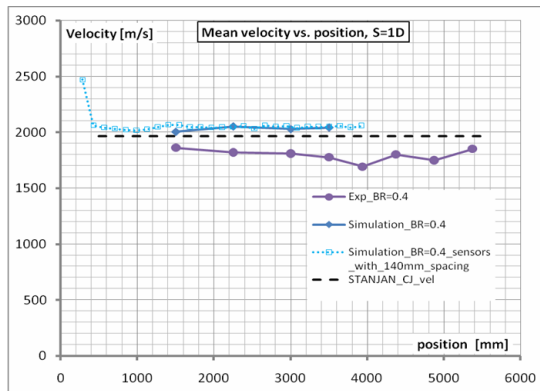


Figure 12: Comparison between experimental and numerical results of velocity

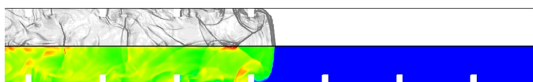


Figure 13: Density gradient and temperature plots for  $\tau = 305.0 \mu s$

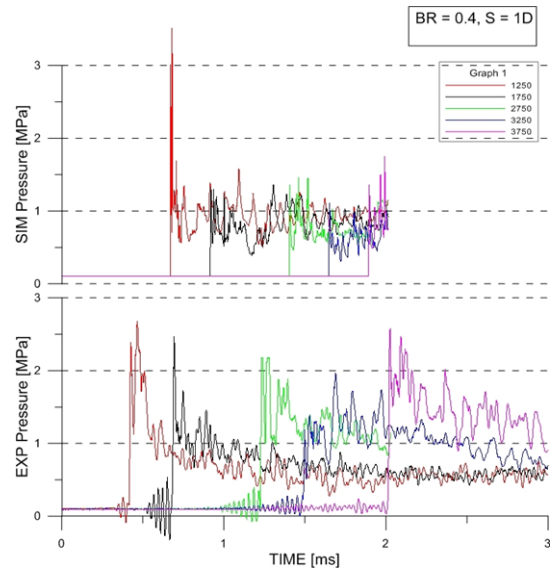


Figure 14: Comparison between experimental and numerical pressure sensors (time scale for experiments shifted to show comparable range)

tion in stoichiometric hydrogen-air mixtures in 6 m long tube was performed. The tube was filled with obstacles located at different configurations. The initial conditions of the hydrogen-air mixtures were 0.1 MPa and 293 K. Four different cases of obstacle blockage ratio (BR) 0.7, 0.6, 0.5 and 0.4 and three cases of obstacle spacing were used. Results show that spacing between obstacles and BR value have very high influence on detonation velocity stability. The higher the spacing is, the lower differences between velocities are for different blockage ratios. For BR = 0.6 and 0.7 spacing influence on percentage difference in velocity is very high and gives values in range of 6–21%. For Blockage ratio 0.4 and 0.5 the same parameter changes in the range of 3–7%. Performed numerical simulation with DETO2D code shows good conformity with theoretical and experimental values of velocity. Detonation wave propagation, reflection and diffraction at the obstacles seem to be correct qualitatively but sensors indications show unconformity in quantitative comparison. The probable reason of unconformity is the reaction kinetic mechanism used in computations. The next step of numerical study will be the analysis of reaction mechanism influence (reduced and 1-step mechanisms) and simulations with different blockage ratio.

## References

- [1] J. Hebral, J. Shepherd, User guide for detonation cell size measurement using photoshop and matlab, Tech. Rep. Report FM00-6, Explosion Dynamics Laboratory, Caltech (2000).
- [2] <http://www.galcit.caltech.edu/edl/public/cantera/mechs/cti/web/>.
- [3] W. R. Chapman, R. V. Wheeler, The propagation of flame in mixtures of methane and air. part iv. the effect of restrictions in the path of the flame, *Journal of Chemical Society* (1926) 2139–2147.
- [4] S. Dorofeev, V. Sidorov, M. Kuznetsov, I. Matsukov, V. Alekseev, Effect of scale on the onset of detonations, *Shock Waves* 10 (2000) 137–149.
- [5] M. Kuznetsov, G. Cicarelli, S. Dorofeev, V. Alekseev, Y. Yankin, T. H. Kim, Ddt in methane-air mixtures, *Shock Waves* 12 (2002) 215–220.
- [6] J. Lee, On the transition from deflagration to detonation, in: *Dynamics of explosions; International Colloquium on Dynamics of Explosions and Reactive Systems*, 10th, Berkeley, CA, USA, 1986, pp. 3–18.
- [7] J. H. S. Lee, *The Detonation Phenomenon*, Cambridge University Press, 2008.
- [8] J. H. S. Lee, I. O. Moen, The mechanism of transition from deflagration to detonation in vapor cloud explosions, *Progress in Energy and Combustion Science* 6 (4) (1980) 359–389.
- [9] K. Shchelkin, Occurrence of detonation in gases in rough-walled tubes, *Soviet Journal of Technical Physics* 17.
- [10] K. Shchelkin, Influence of tube roughness on the formation and detonation propagation in gas, *Journal of Experimental and Theoretical Physics* 10 (1940) 823–827.
- [11] J. Shepherd, J. Lee, On the transition from deflagration to detonation, in: P. Hussaini, P. Kumar, P. Voigt (Eds.), *Major research topics in combustion*, Springer-Verlag, 1992.
- [12] A. Teodorczyk, Deflagration to detonation transition, in: J. Jarosinski, B. Veyssiere (Eds.), *Combustion Phenomena*, CRC Press Taylor & Francis Group, 2009.
- [13] A. Teodorczyk, J. Lee, R. Knystautas, Propagation mechanisms of quasi-detonations, *Proceedings of the Combustion Institute* 22 (1988) 1723–1731.
- [14] P. A. Urtiew, A. K. Oppenheim, Experimental observations of the transition to detonation in an explosive gas, *Proceedings of the Royal Society of London. Series A, Mathematical and Physical Sciences* 295 (1440) (1966) 13–28.